Efficient Antenna Design of Inductive Coupled RFID-Systems with High Power Demand

Christian Reinhold*/**, Peter Scholz*/**, Werner John**, Ulrich Hilleringmann*
*University of Paderborn, Department of Electrical Engineering, Sensor Technology Group, Germany
**Fraunhofer IZM, Departement Advanced System Engineering, Paderborn, Germany
Email: {reinhold, peter.scholz, john}@pb.izm.fraunhofer.de, hilleringmann@ieee.org

***Abstract*— In contrast to pure identification labels, passive inductive coupled RFID transponders with enhanced functionality have an increased power consumption. A non-optimized antenna design for high power transponders may lead to a poor efficiency and high magnetic field emissions. Therefore, in this work, the energy transmission of inductive coupled systems is investigated, enabling an optimized system design. The RFID system is modeled by network elements in order to optimize the energy transmission. Next to a brief review of different methods for the antenna parameter determination, a new modification of the PEEC method is derived enabling an accelerated and accurate computation of the mutual coupling of the reader and the transponder antenna. Along with the simplification of the transformed transponder impedance and the investigation of the reader matching, consecutive design steps are deduced. The influence of the location-dependent antenna coupling on the energy transmission is characterized. Two case studies are carried out showing a successful transmission of 80 mW over a distance of up to 7.6 cm by 275 mW reader output power. This system demonstrates an efficient energy supply of a high power transponder while keeping the field emissions low.**

***Index Terms*— RFID System, Antenna Design, Inductive Coupling, Wireless Energy Transmission, Quality Factor, Inductance Calculation, PEEC**

I. INTRODUCTION

RFID (Radio Frequency IDentification) systems succeed in replacing bar code systems in the supply chain management. Besides of the ability to read out tag information without a line of sight, other applications arise requiring additional functionality of the tag. Especially inductive coupled RFID systems turn out to be adequate because of their potential for an efficient energy transmission.

There is a growing interest in monitoring object related information like temperature, acceleration or pressure [1], [2]. Other applications aim to enhance the label functionality by optical devices like image sensors [3] and displays [4]. Compared to pure identification applications, the energy demand of these so called smart label applications is higher. However, the emission of the electromagnetic field has to stay below regulation boundaries. In order to guarantee an efficient and reliable energy supply while fulfilling the regulations, the energy transmission via the inductive coupled antenna system has to be understood.

Significant work on this topic has been done in the area of medical implants. In [5] the inductive energy transmission was investigated in order to provide energy to an auditory prosthesis taking displacement tolerances into account. In [6] the power transmission for an implanted biomedical device is enhanced in terms of optimizing the coupling coefficient of two spiral coils.

In contrast to medical implants, the situation regarding RFID smart labels is different. The variation of the inductive coupling of the coils of a smart label system caused by changes in the alignment is stronger compared to medical implants in most cases. For this reason, [7] presents an adaptive matching network providing an adequate matching of the reader for varying coupling conditions in order to maximize the power transmission while neglecting efficiency aspects.

In this paper a design approach on the bases of [8], [9] is presented which enables efficient and emission minimized antenna design. The focus of this contribution is on modeling, analyzing and optimizing of the energy transmission via the inductive coupled link.

In section II an overview of the RFID system model is given. For a correct model, it is essential to extract the network element parameters accurately. Different approaches are presented in section III allowing for the computation of the antenna parameters for different scenarios. An adaptation of the PEEC (Partial Element Equivalent Circuit) method is derived which enables a fast and accurate extraction of the positional and angular varying mutual inductance for typical RFID antenna setups.

In order to optimize the energy transmission, a holistic approach is carried out taking the reader and the transponder into account as well as the interaction between each other. In order to give an intuitive interpretation of the system behavior, the transformed transponder impedance is introduced in section IV and simplified by introduction of the frequency deviation. The maximization of the quality factor and the optimization of the coupling are discussed. The matching of the reader antenna is analyzed revealing a single turn reader antenna to be optimum with respect to the data transmission. The gained findings are summarized in a consecutive system design approach.

In section V the influence of the varying coupling coefficient on the energy transmission is analyzed. Case studies are investigated in section VI in order to prove the applicability of the presented concepts by diverse measurement setup scenarios. The key findings of the work are finalized by a conclusion.

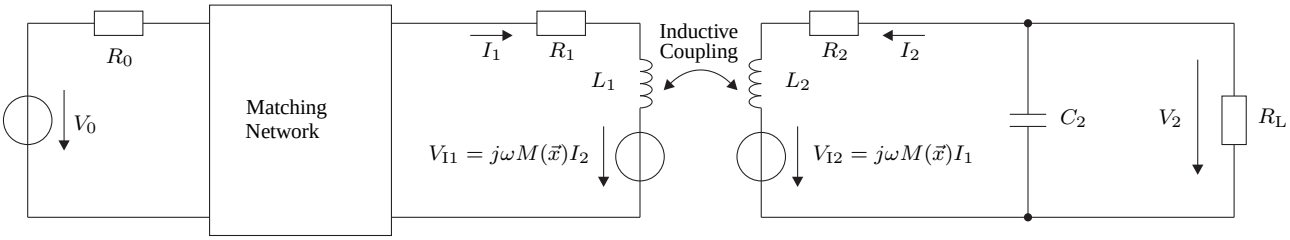

Figure 1. System model of an inductive coupled RFID System

II. Modeling of the RFID System

An RFID system can be separated into two parts: the interrogator and the transponder. An equivalent network[1] is presented in Figure 1.

The reader has to provide the power from a source to an antenna. In the presented model the output stage of the reader is represented by a voltage source V_0 with an internal resistance R_0. To deliver maximum power to the antenna, the impedance of the source has to be matched to the antenna impedance. The antenna can be modeled by an inductance L_1 and a series resistance R_1 in order to take ohmic losses into account. The transponder antenna is modeled in the same way by an inductance L_2 and a resistance R_2. The transponder impedance is tuned to the resonance frequency by a capacitance C_2. The transponder load is modeled by a resistance R_L. The quantity of the load resistance can be determined via the power consumption of the transponder P_req and the requirements to the DC supply voltage V_DD by $R_\mathrm{L} = V_\mathrm{DD}^2/P_\mathrm{req}$.

The inductive coupling is represented by the mutual inductance M which induces a voltage in the transponder V_{I2} due to a current I_1 in the reader coil and vice versa.

III. Inductive Coupled Coils

In this work, the inductive coupled coils are modeled by the self inductances, mutual inductances and resistances.[2] This section describes the computation of these parameters by analytical expressions as well as numerical methods. In section III-A various analytical equations for calculation of the antenna parameters are reviewed as well as important coherences that are needed for this work. A brief overview of different numerical methods is given in III-B. Afterwards a modification of the PEEC method is derived allowing for the effective calculation of the mutual inductance between two rectangular coils. This particular approach is compared with the software tool FastHenry [10].

A. Analytic Expressions

Several analytic equations exist for the calculation of the self inductance of simple shaped coils [11]–[14]. Most approximation expressions are valid for circular or rectangular coils only. Even though these expressions are not feasible for an accurate inductance calculation of complicated coil structures, a general system analysis can be done.

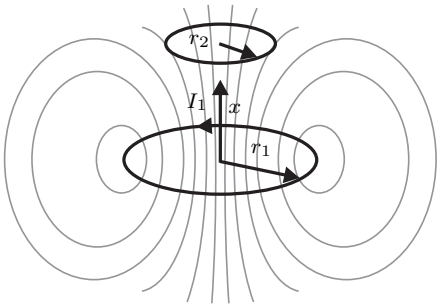

Figure 2. Representation of two inductive coupled coils

For a circular single turn coil as presented in Figure 2, the inductance can be calculated according to [11] by

$$L_0 = \mu_0\, r\, \ln\left(\frac{2\,r}{d}\right), \tag{1}$$

with the permeability of free space μ_0, the coil radius r and the coil wire diameter d. This inductance can be used for the calculation of the inductance of a multi turn inductor by

$$L = N^2\, L_0, \tag{2}$$

where N denotes the number of turns. This equation offers a proper approximation for a cylindrical inductor. In the case of spiral inductors it can be used for general parameter studies. A more precise inductance computation of spiral inductors is given in [15].

Besides of the self inductance, the mutual inductance of two coupled coils is an important figure of merit. It can be calculated analytically for simple coil geometries. The mutual inductance of two coupled circular coils as presented in Figure 2 can be calculated by [11]

$$M = \frac{\mu\pi\ N_1 N_2\ r_1^2 r_2^2}{2\sqrt{\left(r_1^2 + x^2\right)^3}}. \tag{3}$$

In this equation, N_1 and N_2 represent the number of turns of the first and the second inductor respectively. The coil diameters are given by r_1 and r_2 and the axial separation is represented by x. It is important to note that (3) is valid only if the magnetic field created by a current I_1 in the first coil is homogenous in the area bounded

[1] This model does not describe the transient behavior of the transponder. This aspect can be taken into account by regarding the quality factors of the resonant circuits for different load resistances.

[2] Parasitic capacitance of the transponder coil is included in the resonance capacitance C_2.

by the second coil. Therefore the equation is only valid if $r_2 < r_1 \ll x$. A more general approach of calculating the mutual inductance of cylindrical coils with parallel alignment and an arbitrary position is presented in [16].

The coupling of two coils can be expressed by the coupling factor which relates the mutual inductance to the self inductances in the following way

$$k = \frac{M}{\sqrt{L_1 L_2}}. \tag{4}$$

If the coupling factor equals one, the coupling is at maximum while a coupling factor of zero describes two uncoupled coils.

The inductance matrix can be defined in order to calculate the induced voltages from the currents by

$$\boldsymbol{V_1} = j\omega \boldsymbol{L}\, \boldsymbol{I} = j\omega \begin{bmatrix} L_1 & M \\ M & L_2 \end{bmatrix} \begin{bmatrix} I_1 \\ I_2 \end{bmatrix}, \tag{5}$$

with the definitions of the currents and inductances as shown in Figure 1.

The ohmic losses of a coil for DC currents are defined by

$$R_{\mathrm{DC}} = \frac{l}{\sigma A}, \tag{6}$$

where l is the conductor length, A the conductor cross section area and σ the conductivity of the conductor material. The resistance of an N-turn coil can be approximated by $R = N\, R_0$, where R_0 is the resistance of a single-turn coil. For AC currents, the skin effect influences the effective area of the cross section. The skin depth is defined by

$$\delta = \sqrt{\frac{2}{\omega \mu \sigma}}. \tag{7}$$

In this equation $\omega = 2\pi f$ is the angular frequency. The conductivity and permeability are represented by σ and μ respectively. In order to compute the effective AC resistance, it can be assumed that the entire current flows in the conductor skin whose thickness is determined by the skin depth. One has to keep in mind that the skin depth is valid only for a single conductor with a circular cross section. In case of a spiral coil, current in the adjacent coil wires causes a magnetic field resulting in an asymmetric current distribution. This effect is visualized in Figure 3. In order to determine the AC resistance accurately, numerical methods have to be applied.

B. Numerical Methods

In case of complex geometries like coupled rectangular spiral inductors no formulas exist for calculating the inductance analytically. In this case numerical methods can be applied.

For typical inductive coupled RFID applications the separation of the antennas can become large in comparison to the dimensions of the antenna structures resulting in a small surface to volume ratio. Therefore numerical methods requiring a discretization of the entire volume surrounding the antennas like FDTD (Finite Difference Time Domain) methods generate a high computational effort. In order to guarantee numerical stability, the number of necessary FDTD time steps has to be defined by the dimensions of the discretization requiring a huge number of time steps. Therefore lots of computational work for low frequency problems needs to be done [17].

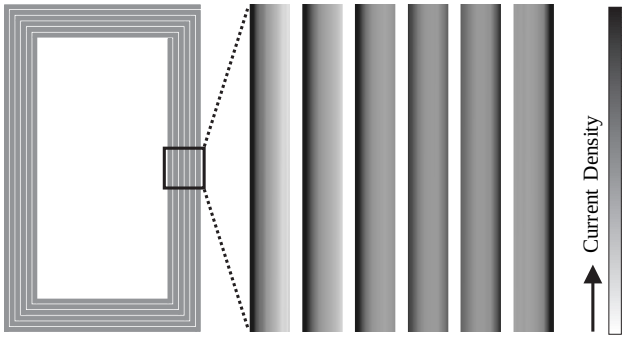

Figure 3. BEM-computed current density of a rectangular spiral inductor.

A further numerical technique to determine the antenna parameters is the BEM (Boundary Element Method). This method requires the discretization of the conductor surface instead of the entire solution space. BEM matrices are typically dense whereas FDTD approaches generate high order sparse matrices with a band structure enabling memory efficient and fast computation.

The PEEC (Partial Element Equivalent Circuit) method represents another numerical antenna parameter computation technique, which has proven applicable for inductive coupled RFID systems. The method presented in [10] can be adapted in order to accelerate the computation of the antenna parameters. This will be explained in the following.

In order to compute the antenna parameters, it is necessary to segment each coil into straight elements. These elements can be split up into parallel brick shaped sections in which a constant current density is assumed. These sections are called filaments in the following. Each filament is defined as being coupled via a partial inductance to all other filaments. The partial inductance can be determined by analytical expressions for an arbitrary arrangement [18]. These partial inductances as well as the filament's resistances are combined to an impedance matrix. By setting up a graph, and thereby defining the filament's connections, it is possible to solve the impedance matrix for the antenna parameters. For a detailed description of the presented approach [10] can be reviewed.

Figure 4 presents two rectangular inductive coupled coils with an arbitrary number of turns. The following derivation will concentrate on the extraction of the mutual inductance M of the two coils by means of the PEEC method. Due to the computational effort, each straight segment is modeled by one filament only. The first N_1-turn rectangular spiral inductor is represented by $P = 4N_1$ branches and the second by $Q = 4N_2$ branches respectively. The total number of branches is $R = P + Q$. The graph, defining the filament's connections, allows for

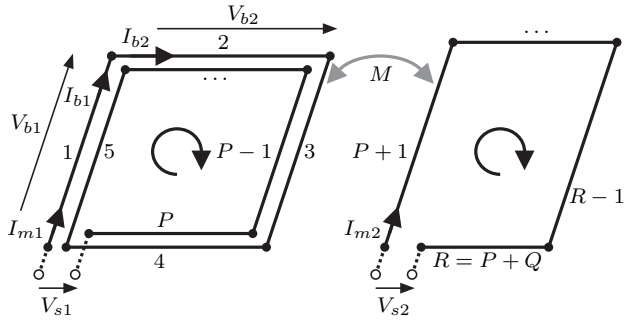

Figure 4. Two inductive coupled segmented inductors

the relation between the branch currents and the branch voltages to be set up by the branch impedance matrix $\boldsymbol{Z}$

$$\boldsymbol{Z}\boldsymbol{I}_b = \boldsymbol{V}_b, \tag{8}$$

where $\boldsymbol{I}_b = [I_{b1}, \ldots, I_{bP}, I_{bP+1}, \ldots, I_{bR}]^T$ is the vector of branch currents and $\boldsymbol{V}_b = [V_{b1}, \ldots, V_{bR}]^T$ is the vector of branch voltages. The impedance matrix is composed as

$$\boldsymbol{Z} = \boldsymbol{R} + j\omega\boldsymbol{L} \ \in \ \boldsymbol{C}^{R\times R}. \tag{9}$$

In this equation $\boldsymbol{R}$ is a diagonal matrix of the DC resistances of each filament according to (6) and $\boldsymbol{L}$ is a dense matrix describing the partial self and mutual inductance of the filaments which may be computed by [18]. In order to extract the impedance for both terminals, it is necessary to set up a mesh matrix[3] $\boldsymbol{M}$, relating the topology of the branches to the ports. Utilizing Kirchhoff's laws yields

$$\boldsymbol{M}\boldsymbol{V}_b = \boldsymbol{V}_s, \quad \boldsymbol{M}^T\boldsymbol{I}_m = \boldsymbol{I}_b, \tag{10}$$

where $\boldsymbol{V}_s = [V_{s1}, V_{s2}]^T$ is the source voltage vector and $\boldsymbol{I}_m = [I_{m1}, I_{m2}]^T$ the port current vector. Combining (8) and (10) results in

$$\boldsymbol{M}\boldsymbol{Z}\boldsymbol{M}^T\boldsymbol{I}_m = \boldsymbol{V}_s. \tag{11}$$

This equation relates the port currents of the two coupled coils to the port voltages. The mutual inductance is represented by element 12 or 21 of the matrix $\boldsymbol{M}\boldsymbol{Z}\boldsymbol{M}^T$, which will be shown in the following.

The matrix $\boldsymbol{M}$ relating the terminal voltages to the branch voltages for two coupled inductors in this case simplifies to

$$\begin{aligned}\boldsymbol{M} &= \begin{bmatrix} M_{11} & \cdots & M_{1P} & M_{1P+1} & \cdots & M_{1R} \\ M_{21} & \cdots & M_{2P} & M_{2P+1} & \cdots & M_{2R} \end{bmatrix} \\ &= \begin{bmatrix} 1 & \cdots & 1 & 0 & \cdots & 0 \\ 0 & \cdots & 0 & 1 & \cdots & 1 \end{bmatrix}. \end{aligned} \tag{12}$$

For the computation of the mutual inductance of the two inductors, it is sufficient to set up (11) with the inductance matrix $\boldsymbol{L}$ and inserting (12)

$$\boldsymbol{M}\boldsymbol{L}\boldsymbol{M}^T = \begin{bmatrix} \sum_{i=1}^{P}\sum_{j=1}^{P} L_{ij} & \sum_{i=1}^{P}\sum_{j=P+1}^{P+Q} L_{ij} \\ \sum_{i=P+1}^{P+Q}\sum_{j=1}^{P} L_{ij} & \sum_{i=P+1}^{P+Q}\sum_{j=P+1}^{P+Q} L_{ij} \end{bmatrix}. \tag{13}$$

[3]Do not mistake the mutual inductance M for the mesh matrix $\boldsymbol{M}$.

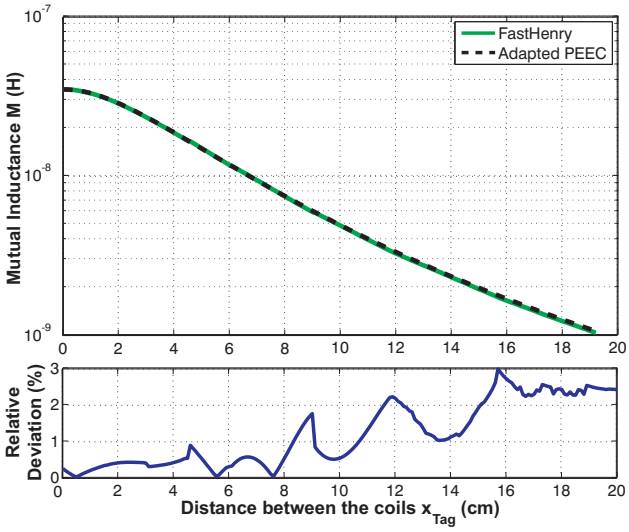

Figure 5. Comparison of the PEEC method implemented in FastHenry according to [10] with each segment separated into 8×2 filaments and the presented adaptation. Parameters are the same as in Figure 14(a).

Comparing (11) and (13) with (5) yields the mutual inductance, that is expressed by element 12 of the matrix in equation (13)

$$M = \sum_{i=1}^{P}\sum_{j=P+1}^{P+Q} L_{ij}. \tag{14}$$

The standard PEEC method presented in [10] demands the solving of an equation system. In contrast to this the modified approach requires the computation of a few partial inductances as well as their summation according to (14), reducing the computational effort.

In Figure 5, the standard PEEC technique is compared with the presented adaptation by calculating the mutual inductance of two parallel coils. The deviation of the two methods does not exceed $3\,\%$.

IV. System Design

In this section a system design approach for an optimum energy transfer is derived. All network element definitions are chosen according to section II and Figure 1. Section IV-A will approximate the transformed transponder impedance, which describes the influence of the transponder on the reader circuit. This approximation allows for easy examination of the parameter influences. In IV-B the tag quality factor is maximized by means of an optimum number of turns for a fixed coil geometry. The antenna geometry is investigated in section IV-C in order to achieve maximum coupling for a given coil separation. In the following section IV-D the matching network of the reader circuit is discussed. The section is concluded by four design steps resulting in an energy efficient system design.

A. Transformed Transponder Impedance

The current of the inductive coupled transponder induces a voltage in the reader antenna. According to [11]

this affect can be modeled via the transformed transponder impedance. It is defined as

$$Z_{\mathrm{T}} = \frac{\omega^2 k^2 L_1 L_2}{Z_{\mathrm{Tag}}} = \frac{\omega^2 k^2 L_1 L_2}{R_2 + j\omega L_2 + \frac{1}{1/R_{\mathrm{L}} + j\omega C_2}}. \quad (15)$$

The reader can be optimized in terms of matching, bandwidth, transferred power etc. when this impedance is known. The transformed impedance is related to many parameters which do not allow an intuitive interpretation. With the following considerations, a simplification of Z_{T} is possible.

With the definitions according to Figure 1, the transponder impedance Z_{Tag} is analyzed

$$Z_{\mathrm{Tag}} = \frac{\frac{R_2}{R_{\mathrm{L}}} + \left(j\omega\frac{L_2}{R_{\mathrm{L}}} + j\omega R_2 C_2\right) - \left[\omega^2 L_2 C_2 - 1\right]}{\frac{1}{R_{\mathrm{L}}} + j\omega C_2}. \quad (16)$$

In order to operate the tag efficiently, the capacitance C_2 is chosen to be resonant with L_2 for $\omega = \omega_0$ by fulfilling $C_2 = 1/(\omega_0^2 L_2)$. The braces of the nominator of (16) can be simplified in the following way

$$(\cdots) = j\frac{\omega}{\omega_0}\left(\frac{\omega_0 L_2}{R_{\mathrm{L}}} + \frac{R_2}{\omega_0 L_2}\right) = j\frac{\omega}{\omega_0} d_2, \quad (17)$$

$$[\cdots] = \frac{\omega^2}{\omega_0^2} - 1 = \frac{\omega}{\omega_0}\left(\frac{\omega}{\omega_0} - \frac{\omega_0}{\omega}\right) = \frac{\omega}{\omega_0}\nu. \quad (18)$$

In (17), d_2 is the damping factor which is related to the quality factor Q_2 by

$$Q_2 = \frac{1}{d_2} = \left(\frac{\omega_0 L_2}{R_{\mathrm{L}}} + \frac{R_2}{\omega_0 L_2}\right)^{-1}. \quad (19)$$

In (18), $\nu = \omega/\omega_0 - \omega_0/\omega$ is the frequency deviation as defined in [5]. Inserting (17) and (18) into (16) leads to

$$Z_{\mathrm{Tag}} = \frac{\frac{R_2}{R_{\mathrm{L}}} + j\frac{\omega}{\omega_0}(d_2 + j\nu)}{\frac{1}{R_{\mathrm{L}}} + j\omega C_2} \approx \omega_0 L_2 (d_2 + j\nu). \quad (20)$$

In the approximation of (20) it is assumed that both, R_2/R_{L} in the nominator and $1/R_{\mathrm{L}}$ in the denominator can be neglected. This is valid because the load resistance R_{L} is far greater in comparison to the coil resistance R_2. By inserting the approximation of (20) into (15) the transformed transponder impedance can be simplified

$$Z_{\mathrm{T,approx}} = \frac{\omega^2}{\omega_0^2}\frac{k^2\,\omega_0 L_1}{d_2 + j\nu}. \quad (21)$$

In order to investigate the validity of the assumptions above, Figure 6 presents a comparison of the simplified formula (21) with the general expression (15) of the transformed transponder impedance. The deviation of the approximation is negligible for optimization aspects where parameter influence is examined.

For the resonance frequency ($\omega = \omega_0$, $\nu = 0$) the transformed transponder impedance from (21) becomes a real value

$$Z_{\mathrm{T,approx},\omega_0} = R_{\mathrm{T}} = \omega_0 k^2 L_1 Q_2. \quad (22)$$

The power dissipated by the tag is[4] $P_{\mathrm{Tag}} = |I_1|^2 R_{\mathrm{T}}$ and

[4]The currents and voltages presented in this paper are interpreted as root-mean-square values.

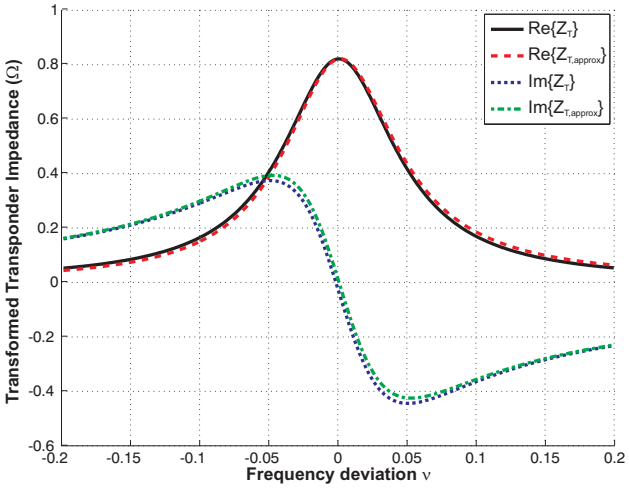

Figure 6. Comparison of (15) and the simplification (21). Parameters are the same as in Figure 11 with $f_0 = 13.56$ MHz and $k = 0.03$.

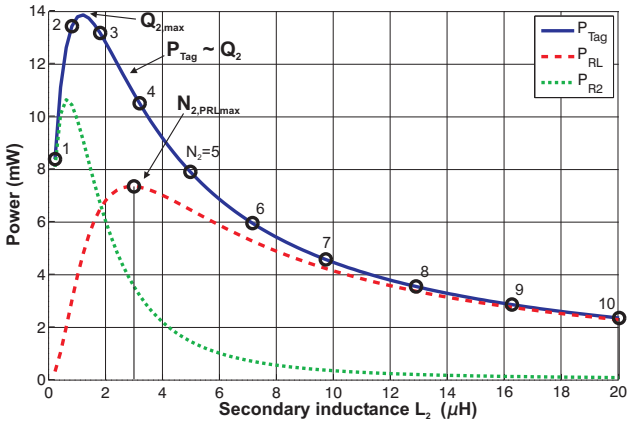

Figure 7. Power and quality factor at the transponder. The quality factor is proportional to the tag power $P_{\mathrm{Tag}} \sim Q_2$. Parameters: $f_0 = 13.56$ MHz, $R_{\mathrm{L}} = 10$ kΩ, $R_{20} = 0.8\ \Omega$, $k = 0.03$, $I_1 = 100$ mA and $L_1 = 0.53\ \mu$H.

therefore linear related to R_{T}. In order to minimize the reader coil current I_1 and the magnetic field emission as well as for a required power delivery, it is necessary to maximize R_{T}. This can be achieved by maximizing Q_2 as well as $k^2 L_1$. For a reliable data transmission, Q_2 is upper bounded due to the bandwidth requirement.

B. Maximization of the Quality Factor

At first, the quality factor Q_2 will be analyzed. The product $k^2 L_1$ is taken into account in the next section.

The tuneable design parameters of Q_2 in (19) are L_2 and R_2. The load resistance R_{L} is determined by the current draw and the supply voltage whereas C_2 is chosen to be resonant with L_2. While maximizing the quality factor by L_2 one has to keep in mind that Q_2 involves two resistances that both dissipate power. For small L_2 the R_2-part dominates and for large L_2 the R_{L}-part respectively (see Figure 7). One has to consider that L_2 and R_2 are dependent on the number of windings N_2.

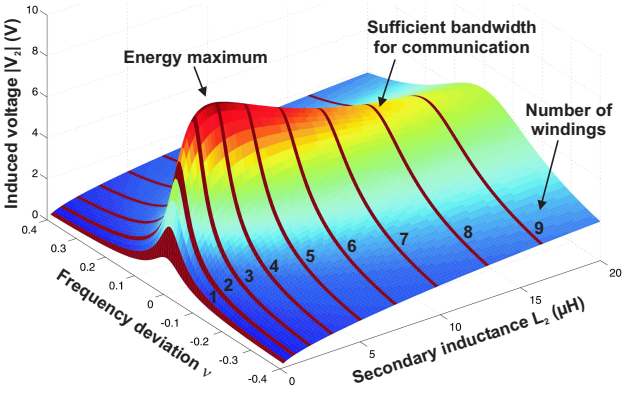

Figure 8. Load voltage V_2 depending on the frequency deviation ν and the inductance L_2. Parameters are the same as in Figure 7.

Due to the fact that it is undesirable to deliver too much power to the coil resistance, the power delivered to the load can be affected by increasing L_2. In order to find the maximum power at the load, one approach is to optimize the load voltage

$$V_2 = \frac{Z_{\mathrm{C_2 \| R_L}}}{Z_{\mathrm{Tag}}} j\omega M I_1 \approx \frac{\omega_0 M\, I_1}{d_2 + j\nu}. \tag{23}$$

In the approximation R_2/R_L in (20) has been neglected. From the voltage V_2, the power transferred to the load can be directly followed by $P_{R_\mathrm{L}} = V_2^2/R_\mathrm{L}$. Figure 8 shows the voltage versus L_2, whereas the results are highlighted at integers of N_2.

In order to find the maximum voltage at the load in dependence of the number of windings N_2, one has to solve the derivation of $\partial V_2/\partial N_2 = 0$. From this follows the optimum turn configuration [8]

$$N_{2,\mathrm{P_{RLmax}}} = \left\lceil \sqrt[3]{\frac{2\, R_{20}\, R_\mathrm{L}}{\omega_0^2\, L_{20}^2}} \right\rceil, \tag{24}$$

where $\lceil \xi \rceil$ denotes that ξ has to be rounded up to the next greater integer.

C. Maximization of the Coupling

The transformed impedance can also be optimized by maximizing $k^2 L_1$ which is the same as maximizing the mutual inductance M, when L_2 is fixed. This can be analyzed by numerical methods e. g. [10] as described above. An example is shown in Figure 9. It can be seen that the optimum reader antenna size varies with the desired readout range.

In order to maximize the transformed impedance, the optimum number of windings of the reader coil has to be investigated as well. Increasing the number of turns N_1 does not improve the power transfer [8]. Instead, regarding the data transmission, it is advisable to use only a single-turn reader antenna in order to keep Q_Reader as low as possible. This aspect will be discussed in the following section.

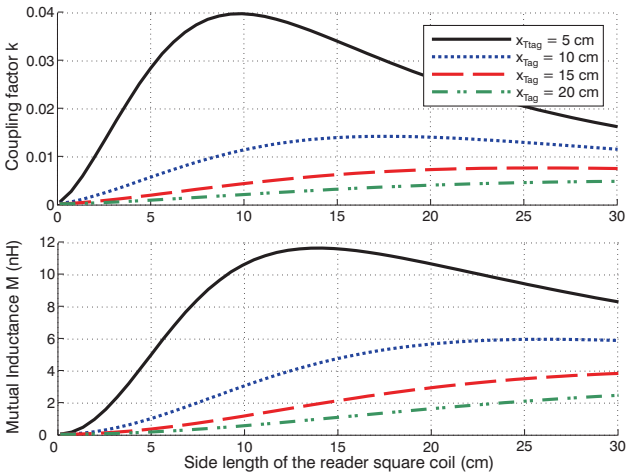

Figure 9. Coupling factor and mutual inductance as a function of the side length of the reader square coil. The side length of the square tag coil is 5 cm. The curves are presented for different tag coil displacements x_Tag.

D. Reader Matching

As presented in Figure 1, the reader antenna has to be matched to the source. An important figure of merit is the quality factor of the matching network. In case of an absent tag ($k = 0$), the quality factor of the primary coil equals

$$Q_{10} = \frac{\omega_0 L_1}{R_1}. \tag{25}$$

If a tag is present ($k \neq 0$) the quality factor becomes

$$Q_{11} = \frac{\omega_0 L_1}{R_1 + R_\mathrm{T}}. \tag{26}$$

Figure 10 shows the matching of the reader for two cases according to (25) and (26).

The total quality factor of the reader circuit is dominated by the Q of the reader antenna highlighted by $R_1 + j\omega_0 L_1$. This is because the related reflection coefficient is placed most close to the border of the Smith Chart which represents an infinite quality factor. The antenna Q can be reduced by a parallel resistor R_p in order to transmit data reliable. For the presented example, by this a quality factor of $Q_{10,R_\mathrm{p}} = 33$ is achieved.

In Figure 10 it can also be seen, that a coupling coefficient of $k \neq 0$ detunes the reader which is matched for the uncoupled case. This mismatch leads to a reduced output power of the source and it can effectuate a poor power transfer for high coupling rates. In order to avoid this effect, the matching network may be designed for a certain coupling factor $k_0 \neq 0$. However, this decreases the readout range, because coupling below k_0 would lead to a mismatch in addition to the low transformed transponder impedance.

In order to achieve the optimum number of windings for the reader coil with consideration of the data transmission, one has to minimize Q_{11}. Because of $L_1 \sim N_1^2$, $R_1 \sim N_1$ and $R_\mathrm{T} \sim N_1^2$ the derivation $\partial Q_{11}/\partial N_1$ reveals that Q_{11} is strictly increasing with N_1. Therefore, in order

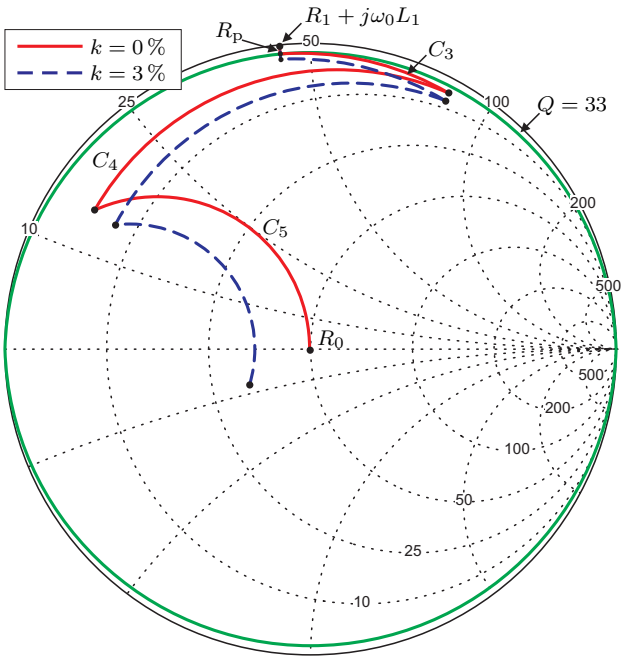

Figure 10. Smith Chart normalized to $50\,\Omega$ with the parameter definitions according to Figure 11.

to keep the reader quality factor as low as possible, a reader coil with $N_1 = 1$ windings should be chosen.

E. System Approach

Summing up the results, a straightforward system design approach can be reached by successively performing the following steps:

1. For a maximum power transfer, the size of the transponder coil should be maximized in order to exploit the available area and maximizing the coupling. This allows for the corresponding base inductance L_{20} and resistance R_{20} to be estimated for an adequate coil wire diameter. The size of the reader coil should be chosen in such a way that $k^2 L_1 = M^2/L_{20}$ is at a maximum for a given spatial arrangement of the coils.
2. For given R_L, L_{20} and R_{20}, an optimum N_2 can be calculated from (24). If the resulting Q_2 is too high for the data transmission, N_2 can be increased at the cost of the energy range.
3. The primary coil should only have one turn in order to keep the Q_1 low. Additionally, the coil resistance R_1 may be increased, for example by thinner circuit wires so as to reduce Q_1. However, this increases the power loss by the coil and decreases the efficiency.
4. If the readout range is the main objective, the reader matching network should be designed for zero coupling ($R_\mathrm{T} = 0$). In this case, scenarios with high coupling ($R_\mathrm{T} \gg 0$) would lead to a mismatch and a poor power transfer. This effect is also known as resonance circuit detuning. Another approach is to design the reader matching network for a certain coupling coefficient k_0. Thus, the efficiency will be at an optimum for this special case, but the borders of functionality will be reduced.

V. Reader Network Matching for Varying Transponder Coupling

The antenna impedance of the reader depends on the coupling coefficient. The resistive part can be expressed with (22) according to Figure 1 as

$$\widetilde{R}_1(k) = R_1 + \omega_0 k^2 L_1 Q_2. \tag{27}$$

If the system is designed for a coupling coefficient k_0, the system is matched for a load $\widetilde{R}_1(k_0)$. Since the reactive elements of the matching network ideally do not dissipate power, the power delivered to $\widetilde{R}_1(k_0)$ is

$$P_{\widetilde{R}_1}(k_0) = P_0 = \frac{V_0^2}{4R_0}. \tag{28}$$

If the transponder coupling k differs from the matched coupling k_0 a mismatch occurs. The mismatch can be characterized by the reflection coefficient

$$\Gamma(k) = \frac{\widetilde{R}_1(k) - \widetilde{R}_1(k_0)}{\widetilde{R}_1(k) + \widetilde{R}_1(k_0)}. \tag{29}$$

Inserting (27) and (25) gives

$$\Gamma(k) = \frac{k^2 - k_0^2}{\frac{2}{Q_{10}Q_2} + k^2 + k_0^2}. \tag{30}$$

The power delivered to the antenna load and to the transponder can be calculated using the the reflection coefficient and the power divider rule by

$$P_{\widetilde{R}_1}(k) = P_{\widetilde{R}_1}(k_0)\left[1 - \Gamma^2(k)\right], \tag{31}$$

$$P_\mathrm{Tag}(k) = P_{\widetilde{R}_1}(k)\,\frac{R_\mathrm{T}}{R_\mathrm{T} + R_1}. \tag{32}$$

The power dissipated by the resistive elements for two test scenarios is presented in the following section.

VI. Case Studies

A test setup according to Figure 11 was utilized in order to verify the results. The challenge was to transmit $80\,\mathrm{mW}$ at about $V_2 = 4.9\,\mathrm{V}$ to the load R_L. Following the four design rules as presented in the previous section, it is necessary to maximize the available area for the tag coil first. In this example, the given size of the tag coil was $6.9\,\mathrm{cm} \times 5.4\,\mathrm{cm}$. According to the numerical simulation, a side length of $12\,\mathrm{cm}$ for the reader coil was chosen so as to reach a power range of less than $10\,\mathrm{cm}$. The arrangement of the test setup is visualized in Figure 14.

Subsequently, the optimum number of windings N_2 and the width of the wires of the tag had to be determined. Since the load $R_\mathrm{L} = (4.9\,\mathrm{V})^2/80\,\mathrm{mW} = 300\,\Omega$ is small in comparison to standard RFID systems, the quality factor of the tag in (19) turns low except if R_2 and L_2 are also small. This was realized by a trace width of $w_2 = 4\,\mathrm{mm}$. By usage of FastHenry [10], $L_{20} = 168\,\mathrm{nH}$ and $R_{20} = 30\,\mathrm{m\Omega}$ were deduced. Referencing to (24),

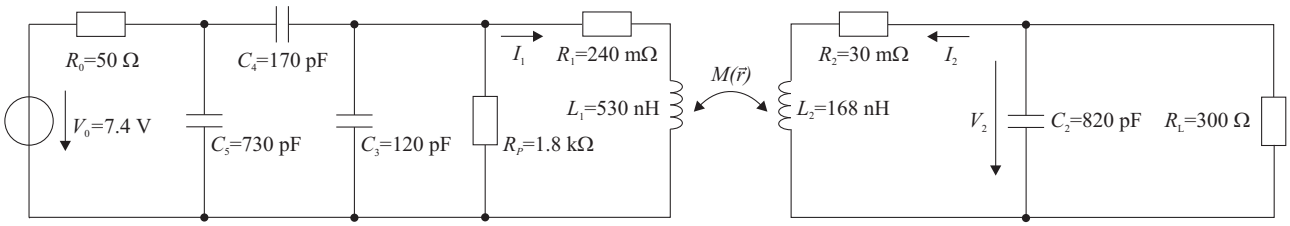

Figure 11. Test setup for transmitting 80 mW to the load R_{L} at $V_2 = 4.9\,\mathrm{V}$.

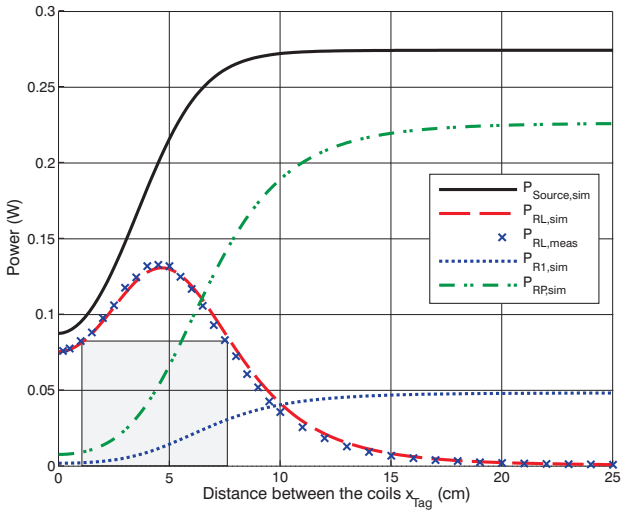

Figure 12. Simulation compared to the measurement for the arrangement of Figure 14(a).

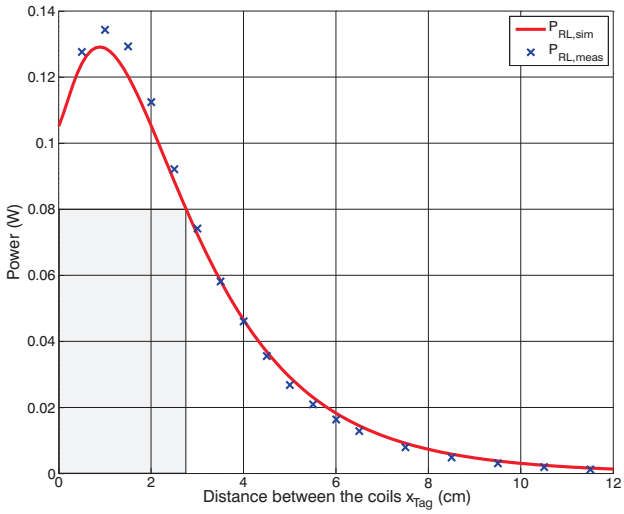

Figure 13. Simulation compared to the measurement for the arrangement of Figure 14(b).

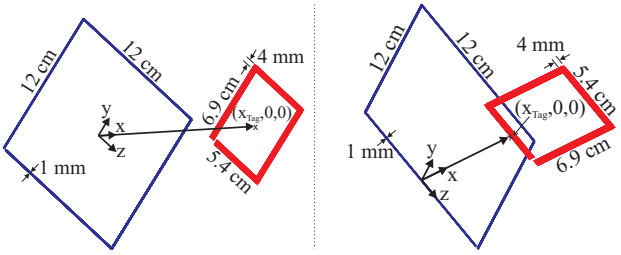

(a) Parallel Arrangement (b) Rectangular Arrangement

Figure 14. Depiction of the spatial arrangements of the reader and transponder coils.

$N_2 = 1$ was chosen. Thus the tag quality factor is $Q_2 = 20$.

In accordance to the third design step, a single winding was chosen for the primary coil. With the trace width of $w_1 = 1\,\mathrm{mm}$, $L_1 = 530\,\mathrm{nH}$, $R_1 = 240\,\mathrm{m\Omega}$ and a quality factor of $Q_1 = 188$ were computed [19]. This high quality factor is unfeasible in respect to a data transmission and could be reduced by thinner trace width of the primary coil. Another possibility to increase the bandwidth is to add a parallel resistor, which is less sensitive towards variations during the manufacturing process. The parallel resistor $R_{\mathrm{p}} = 1.8\,\mathrm{k\Omega}$ reduced the quality factor to $Q_{10,R_{\mathrm{p}}} = 33$.

The reader matching was realized by a Π-matching network consisting of three capacitors (C_3, C_4 and C_5), in order to be able to easily match the primary load to a 50 Ω source. The matching network was designed for the uncoupled system $k_0 = 0$, where $R_{\mathrm{T}} = 0$ [7].

In order to compare the taken measurements with the simulations, both coils were arranged in a parallel direction, with each center points being at $y = 0$ and $z = 0$ (Figure 14(a)). The separation between the tag and the reader coil, indicated by the x-coordinate, was increased from zero to $x_{\mathrm{Tag,max}} = 25\,\mathrm{cm}$, while measurements were taken at the maximum separation of 1 cm per measurement step. The voltage V_2 was measured and the appropriate power was calculated by $P_{\mathrm{RL}} = V_2^2/R_{\mathrm{L}}$.

Figure 12 shows that the measurements match the predicted computations very closely. The power of 80 mW is transmitted at about 1 cm up to 7.6 cm. For large distances, the transformed transponder impedance converges to zero. In this case, the power of the source offered to a 50 Ω load, which is about 275 mW, is parted into the perfectly matched R_{p} and R_1. If the tag is moved closer towards the reader coil, the transformed impedance rises as well as the power at R_{L}. The transformed transponder impedance creates a mismatch that leads to a reduced power output of the source. This effect causes a relatively poor power transfer for small distances.

A second measurement scenario is presented in Figure 14(b). It illustrates the power transmission for a rectangular orientation of the reader and tag. The tag coil was rotated by 90° and moved by x_{Tag}. In Figure 13 simulation results are plotted against measurements. Again, a close correlation is achieved, except for small distances,

where the uncertainty of the position and rotation has a big impact on the coupling factor and therefore on the transmitted power. These errors might be minimized by a more accurate positioning system of the coils. The power of $80\,\mathrm{mW}$ can be transferred at up to $2.7\,\mathrm{cm}$ for a rectangular alignment of the coils. The range can be increased by boosting the power of the source, which results in a shift of the power curve.

With the presented equations, the resulting current I_1 can be calculated. This allows for the computation of the corresponding field strength by numerical field calculation software, in order to show its compliance with EM-field emission boundary legislation.

VII. Conclusion

The presented work focuses on optimizing the antenna system of an inductive coupled RFID system. For this it is important to estimate the antenna parameters. For simple geometries, analytic expressions for the self and mutual inductance as well as the resistance are given. Numerical methods, which can be used for complicated structures are presented and a simplification of the PEEC method for two coupled antennas is developed. The functionality of the simplification is tested by comparing it with the mutual inductance of two coupled rectangular coils for a typical RFID application example. The simplified method results deviate only slightly from the results generated by the original PEEC computation by less than three percent.

In order to give an intuitive interpretation of the influence of the parameters on the energy transmission, the transformed transponder impedance is presented and simplified. Based on this an equation for the optimum turn number is derived. The influence of the coil geometry on the coupling factor is investigated revealing a correlation between the optimum coil geometry and the separation between the reader and the transponder. The presented reader matching considerations result in a single turn reader coil being optimum for the data transmission. The results are summarized in a straightforward step by step design approach. Finally, the influence of a varying transponder coupling on the energy transmission is investigated.

Case studies are carried out to show the power transmission of $80\,\mathrm{mW}$ to a transponder. This power can be achieved by a $275\,\mathrm{mW}$ reader for a rectangular and a perpendicular orientation. The measurement results are in close alignment to the computations based on the system model.

Acknowledgment

The reported R+D work was carried out in the frame of the R+D project PARIFLEX. This particular research was supported by the BMBF (Bundesministerium für Bildung und Forschung) of Republic of Germany under grant 16 SV 2240/16 SV 2239/16 SV 2236. The responsibility for this publication is held by the authors only.

References

[1] H. M. Lu, C. Goldsmith, L. Cauller, and J.-B. Lee, "MEMS-based inductively coupled RFID transponder for implantable wireless sensor applications," *IEEE Transactions on Magnetics*, vol. 43, no. 6, pp. 2412–2414, June 2007.

[2] H.-P. Huang, C.-S. Chen, and T.-Y. Chen, "Mobile diagnosis based on RFID for food safety," in *Proceedings of the IEEE International Conference on Automation Science and Engineering*, October 2006, pp. 357–362.

[3] M. Schwarz, R. Hauschild, B. Hosticka, J. Huppertz, T. Kneip, S. Kolnsberg, W. Mokwa, and H. Trieu, "Single chip CMOS image sensors for a retina implant system," in *Proceedings of the IEEE International Symposium on Circuits and Systems (ISCAS)*, vol. 6, May 1998, pp. 645–648.

[4] W. John, P. Scholz, C. Reinhold, and G. Stönner, "Papierinfoträger haben bald ausgedient," *Funkschau*, vol. 3/2007, pp. 39–41, March 2007.

[5] E. S. Hochmair, "System optimization for improved accuracy in transcutaneous signal and power transmission," *IEEE Transactions on Biomedical Engineering*, vol. BME-31, no. 2, pp. 177–186, February 1984.

[6] S. Atluri and M. Ghovanloo, "A wideband power-efficient inductive wireless link for implantable microelectronic devices using multiple carriers," in *Proceedings of the IEEE International Symposium on Circuits and Systems (ISCAS)*, May 2006, pp. 1131–1134.

[7] B. Jiang, J. R. Smith, M. Philipose, S. Roy, K. Sundara-Rajan, and A. V. Mamishev, "Energy scavenging for inductively coupled passive RFID systems," in *Proceedings of the IEEE Instrumentation and Measurement Technology Conference*, vol. 2, May 2005, pp. 984–989.

[8] P. Scholz, C. Reinhold, W. John, and U. Hilleringmann, "Analysis of energy transmission for inductive coupled RFID tags," in *Proceedings of the IEEE International Conference on RFID*, March 2007, pp. 183–190.

[9] ——, "Antenna design of HF-RFID tags with high power requirement," in *Proceedings of the 19th International Conference on Herzian Optic and Dielectrics (OHD)*, September 2007, pp. 93–98.

[10] M. Kamon, M. J. Tsuk, and J. K. White, "FastHenry: A multipole-accelerated 3-d inductance extraction program," in *Proceedings of the 30th Conference on Design Automation*, 14-18 June 1993, pp. 678–683.

[11] K. Finkenzeller, *RFID Handbook: Fundamentals and Applications in Contactless Smart Cards and Identification*. John Wiley and Sons, 2003.

[12] R. Dengler, "Transponder - Elektrodynamik," pp. 1–9, April 1999.

[13] C. M. Zierhofer, "Geometric approach for coupling enhancement of magnetically coupled coils," *IEEE Transactions on Biomedical Engineering*, vol. 43, no. 7, pp. 708–714, July 1996.

[14] A. Goulbourne, "HF antenna design notes, technical application report," Texas Instruments, Radio Frequency Identification Systems, Tech. Rep. 11-08-26-003, September 2003.

[15] S. Atluri and M. Ghovanloo, "Design of a wideband power-efficient inductive wireless link for implantable biomedical devices using multiple carriers," in *Proceedings of the 2nd International IEEE EMBS Conference on Neural Engineering*, March 2005, pp. 533–537.

[16] L. Hannakam, "Berechnung der gegeninduktivität achsenparalleler zylinderspulen," *Archiv für Elektrotechnik*, vol. 51, pp. 141–154, 1967.

[17] K. S. Yee, "Numerical solution of initial boundary value problems involving maxwells equations," *IEEE Transac-*

tions on Antennas and Propagation, vol. AP-14, no. 3, pp. 302–307, May 1966.
[18] A. E. Ruehli, "Inductance calculations in a complex integrated circuit environment," *IBM Journal of Research and Development*, vol. 16, no. 1, September 1972.
[19] Y. Sun and J. Fidler, "Design of Π impedance matching networks," in *Proceedings of the IEEE International Symposium on Circuits and Systems (ISCAS)*, vol. 5, May 1994, pp. 5–8.

Christian Reinhold was born in Germany in 1978. He received the diploma degree in electrical engineering from the University of Paderborn, Germany in 2005. Since 2006 he has been pursuing the Ph. D. degree at the Sensor Technology Group, University of Paderborn. His current research interests include HF antenna design, energy transmission and near field coupling.

Peter Scholz was born in Germany in 1980. He received the diploma degree in electrical engineering from the University of Paderborn, Germany in 2006. Since 2006 he has been pursuing the Ph. D. degree at the Sensor Technology Group, University of Paderborn. His current research interests include localization of resonant structures, HF antenna design and wireless energy transmission.

Werner John was born in Osnabrueck, on December 13, 1950. He received the Dipl.-Ing. degree from the University of Hanover in 1980. From 1980 to 1985 he was with the University of Paderborn (Department of Electrical Engineering) as a researcher engaged in electromagnetic field theory. From January 1986 to September 1998 he was the head of the group Physical System Design at cadlab(c-lab (joint venture of the University of Paderborn and Siemens Nixdorf Informationssysteme AG). Since October 1998 he has been the head of the Department of Advanced System Engineering at the Fraunhofer Institute of Reliability and Microintegration in Berlin/Paderborn. He is responsible for the development and integration of simulation tools and design methods for Electro Magnetic Reliability (EMR), EMC analysis, EMC engineering, RF design, analogue simulation and design environments. He has 24 years of experience with the development of software (microwave engineering, analogue simulation, EMC and design environment). W. John has authored more than 90 publications in national and international scientific journals and conferences. Since 1888 he served as member and reviewer of the program committees of EMC Zurich, EMC Compo, EMC Europe, EMC Wroclaw, EMV Duesseldorf and Smart Systems Integration.

Ulrich Hilleringmann was born in Germany in 1958. He studied physics from 1978 to 1984 at University of Dortmund, Germany. From 1984 to 1985 he was with the Fraunhofer Institute of Microelectronic Circuits and Systems, Duisburg, Germany. Afterwards Hilleringmann changed to the Department of Electrical Engineering at University of Dortmund, where he wrote a thesis about "Laser Recrystallization of Silicon" in 1988. In 1994 he received the "venia legendi" at the same department with the corresponding thesis "Integrated Optics on Silicon". Since 1999 he has been Professor at the Institute of Electrical Engineering and Information Technology, Sensor Technology Department at University of Paderborn. His main interests are nanometer scale devices, organic electronics, microsystem technologies, RFID and wireless sensors.